Stochastic Wind-Thermal Power Plants Integrated Multi-Objective Optimal Power Flow

Sundaram Bharatbhai Pandya[1*], Hitesh R. Jariwala [2]
1- Department of Electrical Engineering, S.V. National Institute of Technology, Surat, Gujarat 395007, India.
Email: sundarampandya@gmail.com (Corresponding author)
2- Department of Electrical Engineering, S.V. National Institute of Technology, Surat, Gujarat 395007, India.
Email: hrj@eed.svnit.ac.in

Received: November 2019 Revised: February 2020 Accepted: March 2020

ABSTRACT:
The recent state of electrical system comprises the conventional generating units along with the sources of renewable energy. The suggested article recommends a method for the solution of single and multi-objective optimal power flow, incorporating wind energy with traditional coal-based generating stations. In this article, the two thermal power plants are replaced with the wind power plants. The techno-economic analysis are done with this state of electrical system. In proposed work, Weibull probability distribution functions is used for calculating wind power output. A non-dominated sorting based multi-objective moth flame optimization technique is used for the optimization issue. The fuzzy decision-making approach is applied for extracting the best compromise solution. The results are authenticated though modified IEEE-30 bus test system, which is combined with wind and thermal generating plants.

KEYWORDS: Wind Units, Metaheuristics, Stochastic, Probability Density Function.

1. INTRODUCTION

The Optimal Power Flow (OPF) plays a vital role in obtaining regulation and operational management of the electrical grid. The root focus of OPF is to find out the operational region of the electrical network by optimizing the certain objective along with non-violating equality and inequality bounds. It was first introduced by Carpentier [1].

Conventional OPF objective contemplates thermal generating units working by fossil fuels. Due to the growing utilization of renewable energy in the power system, the analysis of OPF is very essential after integrating unpredictability of these non-conventional energy units. OPF considering thermal or coal-based generating units has been broadly analyzed by scientists over the world. Last few years, many stochastic techniques have been proposed in [2-8] for the OPF problem.

While above-mentioned citations consider only classical generating units, an electrical system comprising wind and thermal power units has currently been considered in search of optimum generating cost in some of the articles. Gbest directed Artificial Bee Colony (GABC) is put and used in [9] for the enhancement of OPF outputs obtained in earlier articles using same experimental arrangement. A Modified Bacteria Foraging Approach (MBFA) was proposed in [10]. With Doubly Fed Induction Generator (DFIG) structure in the OPF agenda to express bounds on VAR power production capacity. Another VAR power compensating device, STATCOM (static synchronous compensator) is integrating with [11] for a network having thermal and wind units. Also, the OPF issue was solved with the help of Ant Colony Optimization (ACO) as well as MBFA. Authors in [12] introduced a pattern for the formulation of the cost of wind power. Generators scheduling problem for economic dispatch is a usual problem for a utility having wind power and thermal units. Ref. [13] offered a stochastic model of wind power production. In additional, while solving the similar issue, researchers in [14] involved DFIG model of wind turbine. Article [15] introduced Dynamic Economic Dispatch (DED) structure comprising a wide range of wind energy with risk reserve limits. Ref. [16] included valve-point loading effect of generating unit and emission in DED structure. OPF scheduling system for a solitary hybrid network having solar PV, battery and the diesel generating unit is explained in [17]. Pumped hydro storage is presented in [18] as a substitute storage for the same standalone hybrid network comprising of a wind generating unit, a solar PV, and a diesel generating unit.

Recently, the major challenge in power system is integrating the renewable energy sources like wind power in power grid. The single and multi-objective

optimal power flows, including the renewable energy sources, have attracted the maximum attention.
The author's influence in this paper, are as follows:

- Calculations and modeling of Weibull probability density function comprising the stochastic wind power plants.
- Thermal power plants are replaced with the wind power plants and finally obtain the solution of single and multi-objective OPF problem with the comparative techno-economic analysis. This analysis is devoted to the mathematical modeling of the single and multi-objective OPF problem including complete uncertainty modeling of thermal plants and wind power plants.
- The non-dominated sorting Moth Flame Optimization technique is applied for finding solutions of single and multi-objective OPF problems including stochastic renewable energy sources like wind power and Comparison of results with numerous runs of three newly developed algorithms.

The further sections of the article are arranged as: Section 2 consists of the analysis of mathematical models containing a formulation of uncertainties in solar and wind energy outcomes regarding OPF problem. Section 3 includes discussion on the objectives which is to be optimized. Explanation and application of multi-objective MFO approach are explained in section 4. Numerical results and discussion are presented in section 5 and conclusive notes are given in section 6.

2. MATHEMATICAL MODELS

The elementary information data of modified IEEE-30 bus power system considering the thermal power plants and renewable resources is shown in Table 1. The bus number 5 and bus number 11 are replaced with the wind power plants as displayed in Fig. 1.

Table 1. The main characteristics of the system under study.

Items	Quantity	Details
Buses	30	[19]
Branches	41	[19]
Thermal generators (TG1;TG2;TG3; TG4)	3	Buses: 1 (swing), 2,8 and 13
Wind generators (WG1;WG2)	2	Buses: 5 and 11
Control variables	24	-
Connected load	-	283.4 MW, 126.2 MVAr

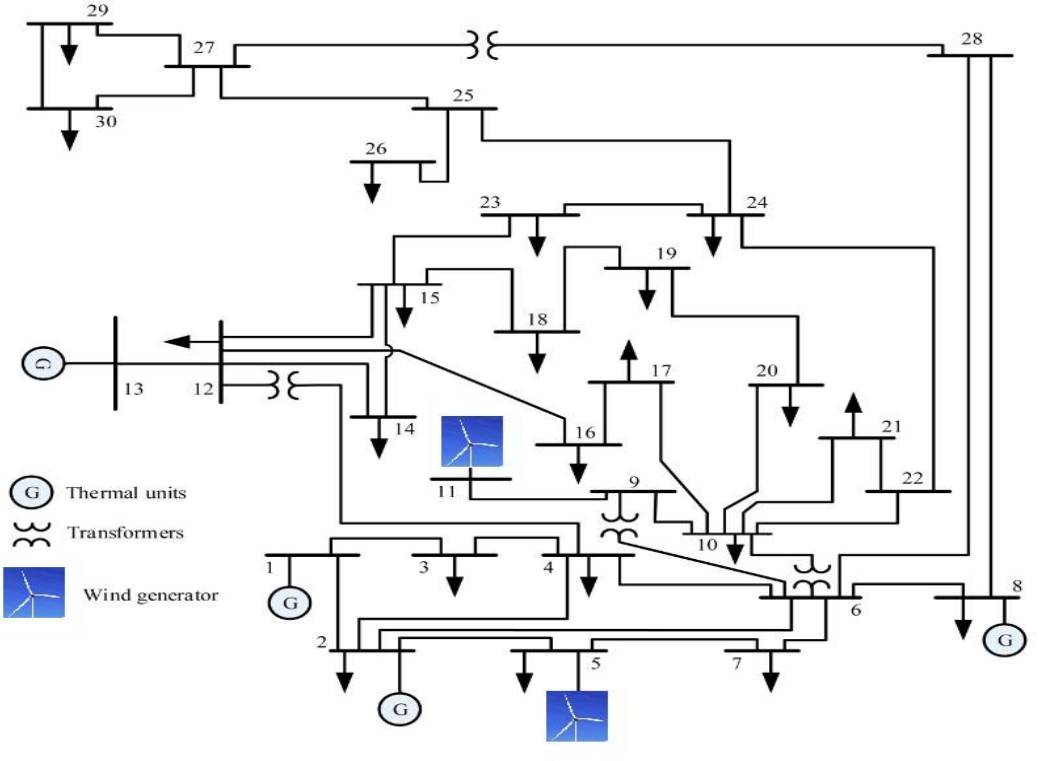

Fig. 1. Modified IEEE 30-bus system with renewable energy units.

All the thermal plants and wind power plants contribute to the total cost of generation. The cost of the conventional thermal generating plants and the renewable sources plants are described in the below section.

2.1. Cost of Thermal Power Units

The thermal generating units operating with the fossil fuels can be figured as the quadratic curve as follows,

$$C_{T0}(P_{TG}) = \sum_{i=1}^{N_{TG}} a_i + b_i P_{TGi} + c_i P_{TGi}^2 \quad (1)$$

Where, a_i b_i and c_i are the cost coefficients for i^{th} thermal power plant. In the real power framework, the generator's fuel cost curves are not simple but they are much intricate and nonlinear in nature. In general, the generation fuel cost function has non-convexity containing numerous swells because of the existence of stacking impacts of the valve point. The ripple effect upon the cost curve is included as redressing sinusoids with quadratic costs. Scientifically, the cost in \$/hr having a valve-point effect is treated as,

$$C_T(P_{TG}) = \sum_{i=1}^{N_{TG}} a_i + b_i P_{TGi} + c_i P_{TGi}^2 + \left| d_i \times \sin\left(e_i \times (P_{TGi}^{min} - P_{TGi})\right)\right| \quad (2)$$

Where, e_i and d_i are the cost coefficients because of valve point effect?

2.2. Emission

The non-renewable energy sources release toxic gases in the atmosphere during power generation. The discharge of NOx and SOx rises with an increase in thermal plants outputs as indicated in Eq. (3). Emission in tones per hour (Ton/hr) can be determined as:

$$\text{Emission } E = \sum_{i=1}^{N_{TG}} \left[(\alpha_i + \beta_i P_{TGi} + \gamma_i P_{TGi}^2) \times 0.01 + \omega_i e^{(\mu_i P_{TGi})}\right] \quad (3)$$

Where, $\alpha_i, \beta_i, \gamma_i, \omega_i$ and μ_i are the emission coefficients with respect to the i^{th} thermal unit. The values of thermal cost coefficients and emission coefficients of thermal power plants are displayed in Table 2.

Table 2. Cost coefficients and emission coefficients of the system under study.

Generator	Bus	a	b	c	d	e	α	β	γ	ω	μ
$TG1$	1	0	2	0.00375	18	0.037	4.091	-5.554	6.49	0.0002	2.857
$TG2$	2	0	1.75	0.0175	16	0.038	2.543	-6.047	5.638	0.0005	3.333
$TG3$	8	0	3.25	0.00834	12	0.045	5.326	-3.55	3.38	0.002	2
$TG4$	13	0	3	0.025	13.5	0.041	6.131	-5.555	5.151	0.0001	6.667

2.3. Direct Cost of Stochastic Renewable Plants

The renewable sources are stochastic in nature and it is very difficult to integrate these sources into the power grid. The wind and solar power units are controlled through the Independent System Operator (ISO). So the private operator has to make the agreement with the grid for a certain amount of scheduled power. The ISO must be sustained the scheduled power. If these renewable farms are not able to maintain the scheduled power, ISO is responsible for the deficiency of the power. Therefore, the spinning reserve supplies the power, if power demand arises. This spinning reserve adds extra cost for the ISO and this condition is termed as overestimation of the renewable sources like wind and solar PV farms. Similarly, in opposite way, if these renewable sources produced more power compared to the scheduled power, it can be wasted because of non-utilization. Therefore, the ISO must tolerate the penalty charge. Thus, the direct cost of the non-conventional units is allied with the scheduled power, overestimation cost because of the spinning reserve and the penalty cost because of the underestimation.

Direct cost related to the wind farms from the j^{th} power plant is modeled with the $P_{ws,j}$ scheduled power from the same sources as,

$$C_{w,j}(P_{ws,j}) = g_j P_{ws,j} \quad (4)$$

Where, g_j indicates the direct cost coefficient and $P_{ws,j}$ is treated as the scheduled power of the j^{th} power plant.

2.4. Uncertain Renewable Wind Power Cost

Owing to the uncertainty of the wind, occasionally the wind farm produces the less amount of the power as compared to scheduled power. Sometimes, it may be possible that actual power provided by wind farm may not satisfy the demand and have lower values. Such power is known as overestimated power by an indeterminate resource. The network ISO should require a spinning reserve to cope up with this type of uncertainty and deliver continuous power source to the end users. The cost of obligating a reserve generator to fulfill the overestimated power is named as reserve cost.

Reserve cost for the j^{th} wind unit is formulated by:

$$C_{Rw,j}(P_{ws,j} - P_{wav,j}) = K_{Rw,j}(P_{ws,j} - P_{wav,j}) = K_{Rw,j}\int_0^{P_{ws,j}}(P_{ws,j} - p_{w,j})f_w(p_{w,j})dp_{w,j} \quad (5)$$

Where, $K_{Rw,j}$ represents a reserve cost coefficient regarding j^{th} wind unit, $P_{ws,j}$ is the definite accessible power from the same unit. $f_w(p_{w,j})$ represents the wind power probability density function for j^{th} wind unit.ae

Opposite to the overestimation condition, it may be possible that the actual power provided by the wind farm is higher from the demand value. Such a scenario is called underestimated power. The leftover power will be lost if there is not any provision for controlling the output power from thermal units. ISO should be paid a penalty charge regarding the excess power.

Penalty charge for the j^{th} wind unit is given by:

$$C_{Pw,j}(P_{wav,j} - P_{ws,j}) = K_{Pw,j}(P_{wav,j} - P_{ws,j}) = K_{Pw,j}\int_{P_{ws,j}}^{P_{wr,j}}(p_{w,j} - P_{ws,j})f_w(p_{w,j})dp_{w,j} \quad (6)$$

Where,$K_{Pw,j}$ represents a penalty cost coefficient of j^{th} wind unit, $P_{wr,j}$ gives the specified output power of the same unit.

2.5. Uncertainty Model of Stochastic Wind Power

In adapted IEEE-30 bus case study, the thermal generating units which are located at bus-5 and bus-11, are replaced by wind power generating units. Data of proposed Weibull shape (k) and scale (c) parameters were displayed in Table 3. Weibull fitting and wind frequency distributions in Fig. 2 and Fig. 3 are achieved by taking 8000 Monte-Carlo scenarios. The Standard given in [19] instructs the design necessity of wind turbines and states maximum turbulent class IA that is verified to operate at highest yearly average wind velocity of 10 meters/sec at hub height. Special focus is for taking shape (k) and scale(c) parameters of wind farms as highest Weibull PDF mean value stuck near 10. In addition, various PDF parameters for two wind farms depict the accurate topographical variety of locations. This is very well known that the distribution of wind speed tracks Weibull Probability Density Function (PDF).

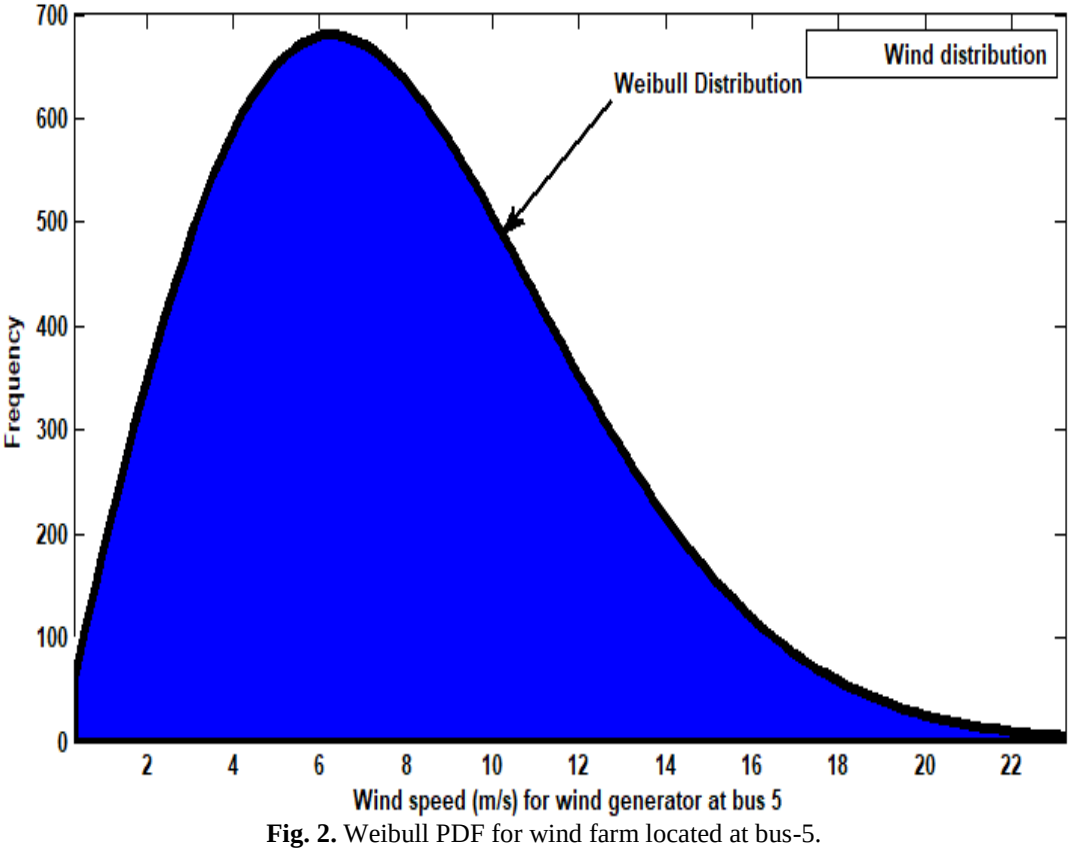

Fig. 2. Weibull PDF for wind farm located at bus-5.

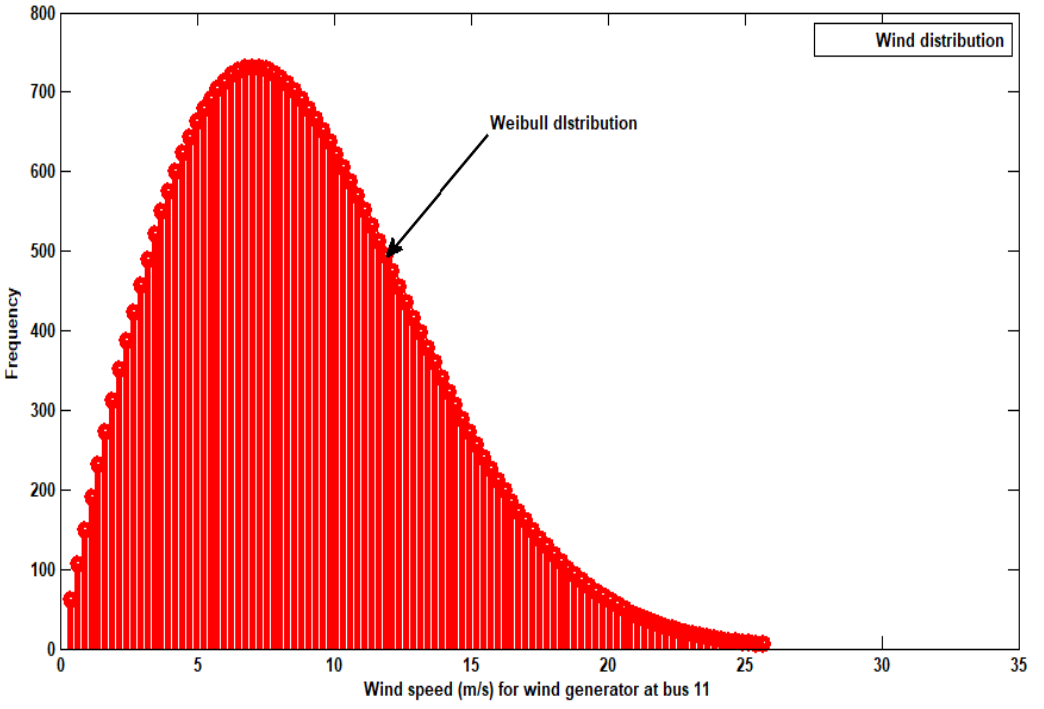

Fig. 3. Weibull PDF for wind farm located at bus-11.

The possibility of wind velocity v meter/sec pursuing weibull PDF including shape factor (k) and scale factor(c) can be calculated as:

$$f_v(v) = \left(\frac{k}{c}\right)\left(\frac{v}{c}\right)^{(k-1)} e^{-\left(\frac{v}{c}\right)^k} \quad for\ 0 < v < \infty \qquad (7)$$

Mean of weibull distribution is stated as:

$$M_{wbl} = c * \Gamma(1 + k^{-1}) \qquad (8)$$

Where, gamma function $\Gamma(x)$ is given by:

$$\Gamma(x) = \int_0^\infty e^{-t} t^{x-1} dt \qquad (9)$$

Table 3. PDF parameters of wind power plants.

Wind power generating plants at Bus-5 and Bus-11.				
Wind farm #	No. of Turbi -nes	Rated power, P_{wr} (MW)	Weibull PDF parameters	Weibull mean, M_{wbl}
1 (bus 5)	25	75	c = 9, k = 2	v = 7.976 m/s
2 (bus 11)	20	60	c = 10, k = 2	v = 8.862 m/s

2.6. Wind Power Model

Wind unit coupled at bus number 5 is taken as the additive outputs of 25 turbines in the farm and output of wind farm containing 20 turbines is coupled at bus number 11. The output rating of each turbine is 3 MW. The accurate output of the wind turbine is varying according to the wind velocity. Turbine output power as a function of wind velocity (v) can be expressed by:

$$p_w(v) = \begin{cases} 0, & \text{for } v \ \langle v_{in} and v \rangle \ v_{out} \\ p_{wr}\left(\frac{v - v_{in}}{v_r - v_{in}}\right) & \text{for } v_{in} \leqslant v \leqslant v_r \\ p_{wr} & \text{for } v_r < v \leqslant v_{out} \end{cases} \qquad (10)$$

Where, v_{in}, v_r and v_{out} show the cut-in, rated and cut-out wind velocity of turbine respectively. p_{wr} shows the rated value of the generated power of the wind turbine. For the 3-MW wind turbine, Enercon E82-E4 model datasheet is

referred. The different speeds are $v_{in} = 3$ metre/sec, $v_r = 16$ metre/sec and $v_{out} = 25$ metre/sec.

2.7. Calculation of Wind Power Probabilities

From Eq. (10), it can be seen that the uncertain wind generation is distinct in some of the spans of wind speeds. If the wind speed (v) is more than the cut-out speed (v_{out}) or less than the cut-in speed (v_{in}), the generated power would be zero. So, the turbine provides rated generated power p_{wr} in the range of rated wind velocity (v_r) and cut-out velocity (v_{out}). Probabilities of these regions can be expressed by [19]:

$$f_w(p_w)\{p_w = 0\} = 1 - \exp\left[-\left(\frac{v_{in}}{c}\right)^k\right] + \exp\left[-\left(\frac{v_{out}}{c}\right)^k\right] \quad (11)$$

$$f_w(p_w)\{p_w = p_{wr}\} = \exp\left[-\left(\frac{v_r}{c}\right)^k\right] - \exp\left[-\left(\frac{v_{out}}{c}\right)^k\right] \quad (12)$$

The wind output is constant between cut-in velocity (v_{in}) and rated velocity (v_r) of wind. In the probability to the continuous zone can be formulated as [19]:

$$f_w(p_w)\{p_w = p_{wr}\} = \exp\left[-\left(\frac{v_r}{c}\right)^k\right] - \exp\left[-\left(\frac{v_{out}}{c}\right)^k\right] \quad (13)$$

3. OBJECTIVES OF OPTIMIZATION

The optimal power flow contains the objectives of optimal active power dispatch and optimal reactive power dispatch. In this section, the objectives of optimal power flow with wind power plants are incorporated as follows;

3.1. Minimization of Total Fuel Cost Including Renewable Energy Resources

The OPF objective is modeled by integrating each cost function that are discussed earlier. In the first objective, the cost of wind and solar power plants are added to the conventional thermal power plants. While, emission cost is not considered. Next objective function is formulated by including emission cost to analyze the change in generation schedule at the time of imposition carbon tax.

Objective 1: Minimize –

$$F_1 = C_T(P_{TG}) + \sum_{j=1}^{N_{WG}}\left[C_{w,j}\left(P_{ws,j}\right) + C_{Rw,j}\left(P_{ws,j} - P_{wav,j}\right) + C_{Pw,j}\left(P_{wav,j} - P_{ws,j}\right)\right] \quad (14)$$

Where, N_{WG} and N_{SG} represent the no. of wind units and solar PV units in a grid, respectively. Remaining cost parameters are determined from Eq. (2) and Eq. (4)-(6).

3.2. Minimization of Total Fuel Cost Plus Carbon Emission Tax Including Renewable Energy Resources

Nowadays, some of the countries are pressurizing the whole power utility to diminish the carbon discharge to control the global warming [19]. In order to inspire venture in cleaner ways of power such as solar and wind, carbon tax (C_{tax}) is charged on discharged of per unit greenhouse smokes. The emission cost (in $/hr) is denoted by Eq. (3) :

Emission cost, $C_E = C_{tax}E$

Objective 2: Minimize –

$$F_2 = F_1 + C_{tax}E \quad (15)$$

3.3. Minimization of Voltage Deviation with Renewable Energy Resources

Bus voltage is a standout among the highest imperative safety and administration superiority lists. The enhancing voltage profile will be acquired by limiting the deviations in voltage of PQ bus from 1.0 for every unit. The objective function will be given by:

Objective 3: Minimize –

$$F3 = \sum_{i=1}^{N_{pq}}|v_i - 1.0| \quad (16)$$

Where, N_{pq} shows the no. of load (PQ) buses, v_i shows the p.u. the voltage level of i^{th} bus.

3.4. Minimization of Active Power Losses With Renewable Energy Resources

The optimization of real power losses P_{LOSS} (MW) may be computed by:

Objective 4: Minimize –

$$F4 = P_{LOSS} = \sum_{i=1}^{NB} P_{Gi} - \sum_{i=1}^{NB} P_{Di} \quad (17)$$

Where, P_{Gi} and P_{Di} represent the output and dispatch at i^{th} bus; NB shows the number of buses.

3.5. Enhancement of Voltage Stability Index Containing Renewable Energy Resources

The most significant index, which indicates the voltage constancy margin of each bus, is the L_{max} index to preserve the constant voltage within suitable level under normal operating conditions. L-index provides a scalar number for every PQ bus. L_{max} index lies in a span of '0' (no load) and '1' (voltage collapse). The amount of voltage collapse indicator for j^{th} bus is obtained as;

$$L_j = \left|1 - \sum_{i=1}^{N_g} F_{ji}\frac{V_i}{V_j}\right| \quad \forall j = 1,2,\dots\dots,NL \quad (18)$$

$$F_{ji} = -[Y_1]^{-1}[Y_2] \quad (19)$$

Where, Y_1 and Y_2 were the sub-matrices of Y_{BUS}. The objective function of voltage stability enhancement is written by;

$$F5 = L = \max(L_j) \quad \forall j = 1,2,\ldots\ldots,NL \quad (20)$$

3.6. Equality Constraints

Equality bounds are given by power flow equations which shows that both real and imaginary power produced in a system should have satisfied the load demand and losses in the system.

$$P_{Gi} - P_{Di} - V_i \sum_{j=1}^{NB} V_j\left[G_{ij}\cos(\delta_{ij}) + B_{ij}\sin(\delta_{ij})\right] = 0 \forall i \in NB \quad (21)$$

$$Q_{Gi} - Q_{Di} - V_i \sum_{j=1}^{NB} V_j\left[G_{ij}\sin(\delta_{ij}) - B_{ij}\cos(\delta_{ij})\right] = 0 \forall i \in NB \quad (22)$$

Where, $\delta_{ij} = \delta_i - \delta_j$, is the variance in phase angles of voltage among bus i and bus j, NB shows overall buses, P_{Di} and Q_{Di} are real and VAR power demand respectively at i^{th} bus. P_{Gi} and Q_{Gi} are real and VAR outputs respectively of i^{th} bus by either unit (thermal or non-conventional) as applicable. G_{ij} shows the conductance and B_{ij} shows the susceptance between bus j and bus i, respectively.

3.7. Inequality Constraints

Inequality bounds were the operational boundaries of devices and security bounds of lines and PQ buses.

Generator bounds:

$$P_{TGi}^{min} \leqslant P_{TGi} \leqslant P_{TGi}^{max}, i = 1, \ldots..,N_{TG} \quad (23)$$

$$P_{\text{ws,j}}^{min} \leqslant P_{ws,j} \leqslant P_{\text{ws,j}}^{max}, j = 1, \ldots..,N_{WG} \quad (24)$$

$$Q_{TGi}^{min} \leqslant Q_{TGi} \leqslant Q_{TGi}^{max}, i = 1, \ldots..,N_{TG} \quad (25)$$

$$Q_{\text{ws,j}}^{min} \leqslant Q_{ws,j} \leqslant Q_{\text{ws,j}}^{max}, j = 1, \ldots..,N_{WG} \quad (26)$$

$$V_{Gi}^{min} \leqslant V_{Gi} \leqslant V_{Gi}^{max}, i = 1, \ldots..,NG \quad (27)$$

Security bounds:

$$V_{L_p}^{min} \leqslant V_{L_p} \leqslant V_{L_p}^{max}, p = 1, \ldots..,NL \quad (28)$$

$$S_{l_q} \leqslant S_{l_q}^{max}, q = 1, \ldots..,nl \quad (29)$$

Eq. (23) and Eq. (33) signify the real power output bounds of thermal, wind units. Afterward, Eq. (25) and Eq. (26) signify the VAR power capacity of generating units. NG shows the overall voltage control buses. Eq. (27) shows bounds on the voltage of PV buses, whereas, Eq. (28) shows the voltage bounds on PQ buses where NL is the number of PQ buses. Line loading boundaries are defined using Eq. (29) for total nl number of lines in a system.

4. MULTI-OBJECTIVE MOTH FLAME OPTIMIZER

Here, the Moth Flame Optimization (MFO) algorithm is adopted to solve the multi-objective optimal power flow problem.

4.1. Inspiration

It is basically inspired from the moths in nature. The navigation of the moths at night is a little bit interesting by using the moonlight. The transverse orientation of mechanism is utilized by the moths for navigation as shown in Fig. 4. The moth flies by keeping up some point concerning the moon, the vital and viable mechanics of long traveling long separations. Be that as it may, regardless of the transverse orientation, moths fly spirally around the lights as appeared in Fig. 5. This is a direct result of the inadequacy of the transverse introduction, in which it is valuable for suffering in a linear way at the time of remote location light source. Exactly when moths get an artificial light source, they do efforts to keep up a comparative edge to a light source to soar in a linear way. Meanwhile, this light is to an extraordinary degree close stood out from the moon, nevertheless, keeping up the same point at a light source creates a vain or lethal winding to sail route for moths.

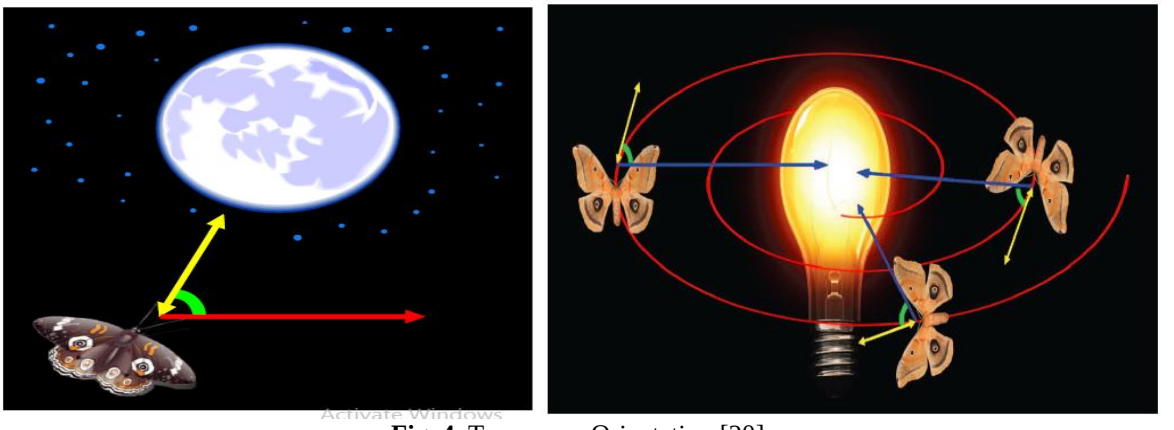

Fig. 4. Transverse Orientation [20].

4.2. MFO algorithm

In MFO algorithm, the solutions of problems are given by moths and the variables are represented by the positions of moths in a space, flying in 1D, 2D, 3D or any other dimensional space by varying its position vectors.

1. Initialize position vector of moths:

With 'n' shows the overall variables and'd' shows the dimensions, the position matrix is given by,

$$M = \begin{bmatrix} m_{1,1} & m_{1,2} & \cdots & m_{1,d} \\ m_{2,1} & m_{2,2} & \cdots & m_{2,d} \\ \vdots & \vdots & \vdots & \vdots \\ m_{n,1} & m_{1,1} & \cdots & m_{n,d} \end{bmatrix} \quad (30)$$

2. Initialize position vector of Flames:

Another valuable matrix is the position vector matrix of flames which is given by;

$$F = \begin{bmatrix} F_{1,1} & F_{1,2} & \cdots & F_{1,d} \\ F_{2,1} & F_{2,2} & \cdots & F_{2,d} \\ \vdots & \vdots & \vdots & \vdots \\ F_{n,1} & F_{1,1} & \cdots & F_{n,d} \end{bmatrix} \quad (31)$$

Where, the 'n' shows overall variables and the'd' shows overall dimensions.

3. Fitness evaluation:

For the finding the fitness, there is an array of the moths which is given by,

$$OM = \begin{bmatrix} OM_1 \\ OM_2 \\ \vdots \\ OM_n \end{bmatrix} \quad (32)$$

Where, 'n' gives the overall value of moths. It may be seen that the dimensions of the position vectors of moths and flames are the same. So the vector for saving the equivalent fitness value is given by,

$$OF = \begin{bmatrix} OF_1 \\ OF_2 \\ \vdots \\ OF_n \end{bmatrix} \quad (33)$$

The MFO approach is having the three main functions for finding the global results as below;

$$MFO = (I, P, T) \quad (34)$$

I illustrates the function for generating the custom populations with the corresponding fitness which is given by,

$$I: \emptyset \rightarrow \{M, OM\} \quad (35)$$

Similarly, P function is also the main function, and getting from the matrix of M eventually updated as;

$$P: M \rightarrow M \quad (36)$$

Also, there is another termination criterion for T function for the condition, satisfaction means if satisfied than true otherwise false.

$$T: M \rightarrow \{TRUE, FALSE\} \quad (37)$$

Firstly, the initialization of the functions, the 'P' function is evaluated until the satisfaction standards of the 'T' function are not fulfilled. Now the moth is modified according to the flame, so the mathematical model of the transverse orientations of this behavior is given by the equation given below;

$$M_i = S(M_i, F_i) \quad (38)$$

Where, M_i indicates the i^{th} moth, F_i indicates the j^{th} moth of the spiral function S. Here, the motion of moth is n logarithmic spiral whose starting point should be the moth, the final point should be flame and a range does not surpass the exploration area. So the point of the MFO approach in logarithmic scale is shown in Fig. 5 and given as follows;

$$S(M_i, F_i) = D_i . e^{bt} . \cos(2\pi t) + F_j \quad (39)$$

Where, D_i is the remoteness of i^{th} moth from j^{th} flame. "b" is the constant indicating the profile of the log spiral and t is the random number in the range of [-1, 1]. The calculation of distance D_i can be given as;

$$D_i = |F_j - M_i| \quad (40)$$

Where, D_i is the remoteness of i^{th}moth from the j^{th} moth, F_j shows the j^{th} flame and M_i shows the i^{th}moth.

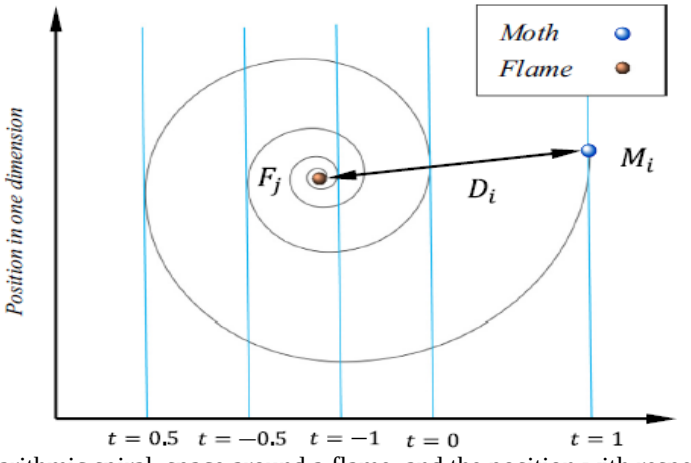

Fig. 5. Logarithmic spiral, space around a flame, and the position with respect to t [20].

4. Adaptive nature of reducing the number of flames:

Further, the numbers of flames are reduced while the number of iterations is increasing which is given by;

$$Number\ of\ flames = round\left(N - I * \frac{N-1}{T}\right) \quad (41)$$

Where, I illustrates the present iteration, N shows the highest number of flames having the overall iterations T.

4.3. Formulation of Multi-Objective Function with the Non-sorting MFO Algorithm

The multi-objective optimization issues comprising the amount of clashing objective functions are optimized simultaneously while at the same time fulfilling all the constraints. There are the number of optimization methods that are utilized prior to the article to explain the multi-objective OPF problem. Starting with those works of literature, it is seen that numerous researchers have changed over that multi-objective issue under a single objective issue utilizing the straight mixture of the two clashing objective works toward applying the weighting components approach. Furthermore, the finer route for finding the result of the multi-objective issue may be to estimate the set of ideal tradeoffs what's more discovering the best compromising solutions around every last one of pareto fronts. The multi-objective optimization problem needs to be figured as;

$$Min\ f_i(u), \quad i = 1,2,3 \dots \dots \dots \dots, N \quad (42)$$
$$Subjected\ to\ g_j(u) = 0, \quad j = 1,2,3 \dots . M \quad (43)$$
$$h_k(u) \leq 0, \quad k = 1,2,3 \dots \dots \dots \dots . K \quad (44)$$

Where, f_i shows the i^{th} objective function; u represents the decision vectors; N stands for total objective function; M stands for the total power flow bounds and K stands for total physical bounds on devices. In the multi-objective optimization, the non-dominated sorting technique can have two probabilities, one dominating the other objectives or no one dominated the other. In other words, without losing generality; u_1 dominates the u_2 only if the given two criteria are fulfilled;

$$\forall i \in \{1,2,3 \dots \dots N\} \quad : f_i(u_1) \leq f_i(u_2) \quad (45)$$
$$\exists j \in \{1,2,3 \dots \dots N\} \quad : f_j(u_1) \leq f_j(u_2) \quad (46)$$

In the event that any of the above conditions is disregarded, at that point, arrangement u_1 does not rule u_2. The arrangement u_1 is known as the non-commanded arrangement, if u_1 overwhelms the u_2 arrangements. Flowchart of given MFO approach for resolving OPF issue is shown in Fig. 6, the method of the suggested non-sorting MFO approach has appeared in algorithm-2. Initially, introduce parameters, for example, population sizeN_{pop}, and stopping value, here it is the most extreme no. of generation to proceed the method. Besides, a random parent population P_o in possible space S is produced and every objective function of the objective vector F for P_o is assessed. Afterward, non-dominated sorting along with crowding distance calculation as clarified in [21] is implemented on P_o. Subsequently, the MFO approach is utilized to make the fresh population P_j, and then it is converged with P_o to shape the blended population P_i. This P_i is arranged in view of elitism non-domination, and in light of the figured estimations of crowding distance (CD) and non-domination rank (NDR), the best N_{pop} arrangements are refreshed to frame another parent population. This procedure is repeated until the highest no. of generations (cycles) are come to. It must be noticed that a similar approach can be utilized along

with end criteria set according to the total evaluations of the function.

Algorithm-2 Non-dominated Moth Flame Optimization [21]

Step 1:-

Create population P_o randomly in the set of solution S and objective function vector F for the created P_o.

Step 2:-

Sort the P_o in light of the elitist non dominated sort strategy and discover the non-domination rank (NDR) and pareto fronts.

Step 3:-

For each pareto front, find the crowding distance (CD).

Step 4:-

Now using MFO algorithm, modernize solutions P_j.

Step 5:-

To create $P_i = P_o \cup P_j$, combine $P_o$andP_j.

Step 6:-

For P_i accomplish step 2 according to NDR and CD sort P_i.

Step 7:-

For first N_{pop} members of P_i, Substitute P_o with P_i.

4.4. Fuzzy Model for the Multi-Objective Problem

For finding the best compromising solution among all the non-inferior results, the fuzzy membership approach can be applied in multi-objective functions. The fuzzy membership function μ_{f_i} is looking after minimum f_i^{min} and maximum f_i^{max} values for every objective goal with the help of fuzzy membership function. Now, the membership function of i^{th} objective is expressed as;

$$\mu_{f_i} = \begin{cases} 1 & f_i \le f_i^{min} \\ \frac{f_i^{max} - f_i}{f_i^{max} - f_i^{min}} & f_i^{min} < f_i < f_i^{max} \\ 0 & f_i \ge f_i^{max} \end{cases} \quad (47)$$

The values of membership functions lie in the scale of (0-1) and show that how much it satisfies the function f_i. Afterward, the decision-making function μ^k should be computed as follows;

$$\mu^k = \frac{\sum_{i=1}^{N} \mu_{f_i}^k}{\sum_{k=1}^{M} \sum_{i=1}^{N} \mu_{f_i}^k} \quad (48)$$

The decision-making function can also be considered as the normalized membership function for non-inferior results and shows the ranking of the non-dominated results. The final result is treated as the best compromising solution among all the pareto front having the value $maximum\{\mu^k: k = 1,2,3 \dots\dots M\}$.

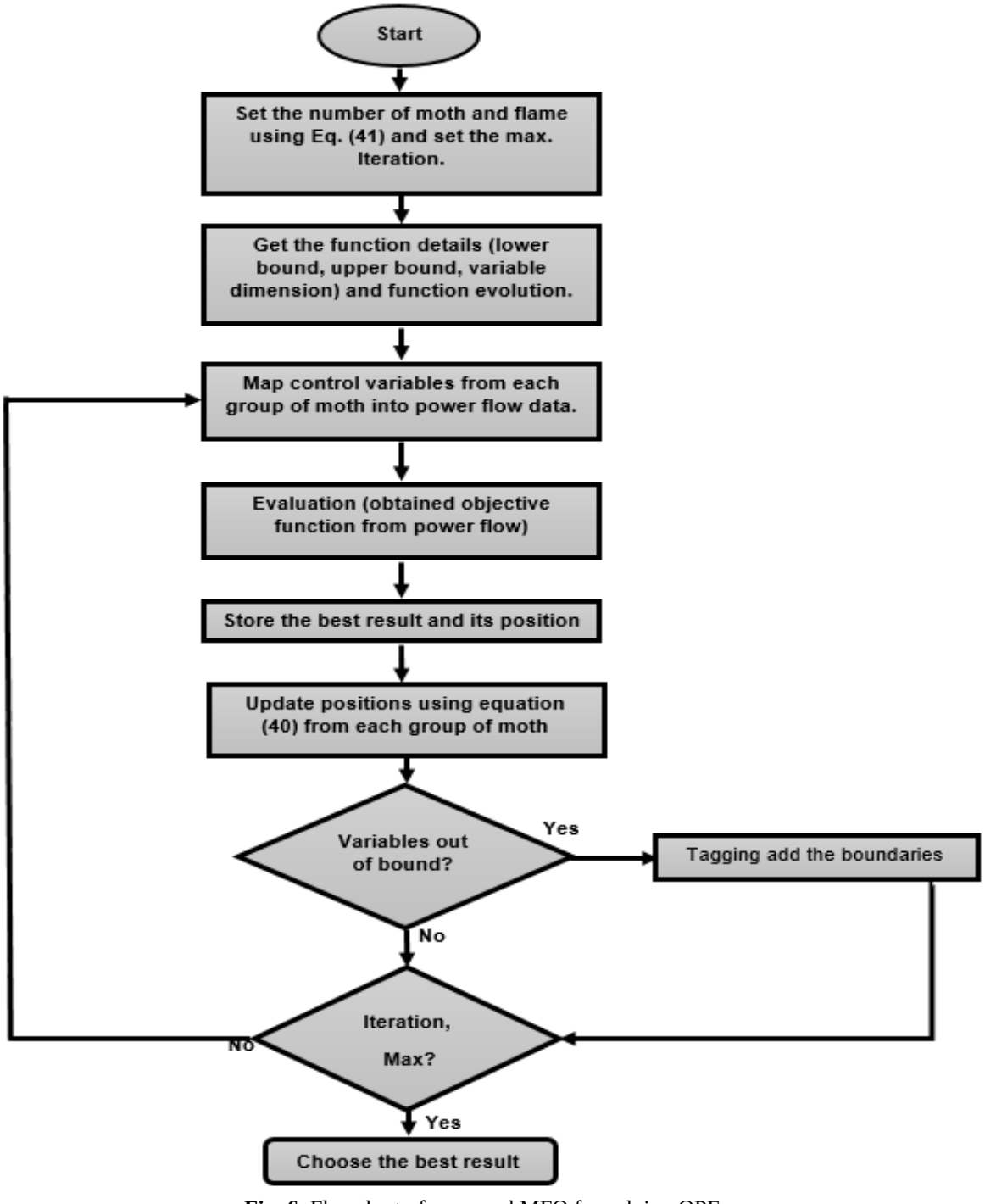

Fig. 6. Flowchart of proposed MFO for solving OPF.

5. SIMULATION RESULTS AND ANALYSIS

In this analysis, the single objective and multi-objective optimization using MFO algorithm are implemented to solve the stochastic OPF problem with wind-thermal power plants. The adapted IEEE-30 bus framework with wind-thermal plants can be utilized to show the adequacy of the suggested approach. The line information, load information and the data of wind and solar power plants are directly taken from ref. [19]. The primary qualities of adapted IEEE-30 bus framework are given in Table 1.

Here, total 11 dissimilar test cases are considered as presented in Table 4. The first six case studies are for single objectives optimization and rest of the cases are multi-objective optimization problems incorporated with thermal and wind power plants. In proposed work,

the programming is done with MATLAB programming language and calculated on the system having 2.5 GHz core to duo processor with 2 GB RAM. Here, the search agent value is choosing to be 40 and each algorithm is analyzed for 10 independent runs with 100 iterations per run.

Table 4. Summary of case studies for adapted IEEE-30 bus test system.

Test system	Case #	Single and Multi Objectives Functions
IEEE 30-bus test system (Modified)	Case # 1	Minimization total fuel cost.
	Case # 2	Emission minimization.
	Case # 3	Active power loss minimization.
	Case # 4	Voltage deviation minimization.
	Case # 5	Voltage stability enhancement.
	Case # 6	Total Fuel Cost with carbon Tax minimization.
	Case # 7	Total Fuel Cost and Emission minimization.
	Case # 8	Total Fuel Cost and active power loss minimization.
	Case # 9	Total Fuel Cost, Emission, and active power loss minimization.
	Case # 10	Total Fuel Cost, Emission, and voltage deviation minimization.
	Case # 11	Total Fuel Cost, Emission, Voltage deviation and active power loss minimization.

. 5.1. Scenario-1 (Single objective OPF with wind-thermal power plants)

Here, all the objectives are treated as the single objectives and optimized with the help of moth flame optimization algorithm. The best optimized results are tabulated in Table 5 to Table-7. For Case-1, the total fuel cost including renewable wind power plants as in case-1 is **669.523 $/hr.** The convergence curve of total fuel cost with all four algorithms is displayed in Fig. 7. The pollutant gas emission in case-2 is **0.092 Ton/hr.** The active power loss of different transmission lines in case-3 is **1.747 MW**. Likewise, the voltage deviation of each bus that is case-4, the minimum value is **0.294 p.u.** The voltage stability index, also known as L_{max} index fluctuates from 0 (no load) to 1 (voltage collapse). So the minimum value for the L_{max} index in case-5 is **0.134**. In case-6, the carbon tax rate C_{tax} is taken as **20 $/Tonne**. The simulation result of total cost with emission is **697.703 $/hr.** After comparing the simulation outcomes with three newly developed algorithms, it shows that the proposed MFO algorithm is well applied for the OPF Problem with the wind-thermal power plants.

Table 5. Single objectives simulation results for case-1 and case-2 (Adapted IEEE 30 bus system).

Control & State variables	Min	Max	Case-1				Case-2			
			MFO	GWO	MVO	IMO	MFO	GWO	MVO	IMO
PG2(Thermal)	**20**	**80**	24.906	26.884	25.433	38.227	46.634	46.607	46.609	47.373
PG5(Wind)	**0**	**75**	42.010	42.247	42.907	22.701	74.921	71.362	73.825	75.000
PG8(Thermal)	**10**	**35**	10.000	10.000	10.054	15.577	35.000	35.000	35.000	35.000
PG11(Wind)	**0**	**60**	37.064	35.034	35.669	38.368	58.454	60.000	59.283	55.124
PG13(Thermal)	**12**	**40**	40.000	40.000	40.000	39.993	39.999	39.366	38.065	39.319
VG1	**1.10**	**0.95**	1.100	1.100	1.099	1.100	1.100	1.077	1.011	1.100
VG2	**1.10**	**0.95**	1.089	1.007	1.090	1.100	0.950	0.958	1.080	1.100
VG5	**1.10**	**0.95**	1.069	1.067	1.098	1.100	0.950	1.030	1.073	1.100
VG8	**1.10**	**0.95**	1.091	1.099	1.099	1.100	1.082	1.077	1.009	1.100
VG11	**1.10**	**0.95**	1.100	1.099	1.098	1.100	0.998	1.098	1.013	1.100
VG13	**1.10**	**0.95**	1.095	1.086	1.067	1.068	0.986	1.093	0.957	1.100

QC10	**5.00**	**0.00**	5.000	1.857	0.316	5.000	5.000	1.791	0.812	5.000
QC12	**5.00**	**0.00**	4.490	1.857	0.437	3.649	5.000	4.821	4.985	5.000
QC15	**5.00**	**0.00**	0.746	2.024	2.945	5.000	0.546	3.520	3.599	5.000
QC17	**5.00**	**0.00**	0.000	0.036	0.881	5.000	3.024	1.080	1.112	2.981
QC20	**5.00**	**0.00**	0.010	1.048	2.595	0.979	4.162	4.750	4.995	5.000
QC21	**5.00**	**0.00**	4.298	1.361	4.732	3.113	0.012	2.162	3.677	5.000
QC23	**5.00**	**0.00**	4.867	0.596	1.072	5.000	2.746	3.433	2.870	0.513
QC24	**5.00**	**0.00**	4.990	3.218	4.952	4.298	0.001	0.263	0.133	5.000
QC29	**5.00**	**0.00**	5.000	0.042	2.464	2.389	5.000	0.743	4.455	5.000
T11(6-9)	**1.10**	**0.9**	1.099	1.100	0.909	1.100	0.900	1.092	0.932	1.100
T12(6-10)	**1.10**	**0.9**	1.074	0.929	0.939	1.100	1.100	1.077	0.936	1.100
T15(4-12)	**1.10**	**0.9**	0.931	0.958	0.938	1.100	1.099	1.100	0.909	1.100
T36(28-27)	**1.10**	**0.9**	0.901	1.100	0.910	1.100	0.900	0.928	1.017	1.100
Total Fuel Cost ($/hr)			**669.523**	**669.942**	**669.722**	**687.804**	**-**	**-**	**-**	**-**
Emission (Ton/hr)			**-**	**-**	**-**	**-**	**0.092**	**0.092**	**0.092**	**0.092**

Table 6. Single objectives simulation results for case-3 and case-4 (Adapted IEEE 30 bus system).

Control & State variables	**Min**	**Max**	**Case-3**				**Case-4**			
			MFO	**GWO**	**MVO**	**IMO**	**MFO**	**GWO**	**MVO**	**IMO**
PG2(Thermal)	**20**	**80**	65.254	77.746	72.026	65.756	22.328	39.173	69.326	79.321
PG5(Wind)	**0**	**75**	75.000	75.000	74.829	75.000	0.000	57.618	73.328	42.434
PG8(Thermal)	**10**	**35**	35.000	35.000	35.000	35.000	34.995	19.456	26.076	33.141
PG11(Wind)	**0**	**60**	60.000	59.898	59.695	60.000	17.067	39.698	25.180	12.290
PG13(Thermal)	**12**	**40**	40.000	40.000	40.000	40.000	12.000	12.070	15.651	13.112
VG1	**1.10**	**0.95**	1.100	1.029	1.100	1.100	0.973	0.961	0.983	1.063
VG2	**1.10**	**0.95**	1.100	1.100	1.100	1.100	0.955	0.952	0.950	0.983
VG5	**1.10**	**0.95**	1.090	1.090	1.092	1.100	1.100	1.003	1.040	1.021
VG8	**1.10**	**0.95**	1.095	1.092	1.093	1.100	1.091	1.067	1.036	1.084
VG11	**1.10**	**0.95**	1.100	1.100	1.100	1.100	1.100	1.100	1.069	1.095
VG13	**1.10**	**0.95**	1.098	1.100	1.100	1.100	1.054	1.071	1.091	1.095
QC10	**5.00**	**0.00**	4.959	0.056	3.255	5.000	0.690	1.640	2.734	4.335
QC12	**5.00**	**0.00**	3.710	3.006	1.018	5.000	4.998	0.370	3.246	3.420
QC15	**5.00**	**0.00**	1.191	1.030	0.555	5.000	0.260	1.252	3.439	0.316
QC17	**5.00**	**0.00**	5.000	0.317	0.113	5.000	3.294	3.891	1.861	2.887
QC20	**5.00**	**0.00**	4.992	2.391	1.687	5.000	0.000	1.926	0.776	2.210
QC21	**5.00**	**0.00**	1.816	0.185	2.817	5.000	4.964	4.132	2.589	2.733
QC23	**5.00**	**0.00**	0.000	0.000	4.867	5.000	4.999	0.258	2.416	2.166
QC24	**5.00**	**0.00**	3.415	0.434	3.975	5.000	3.153	3.151	4.769	1.750
QC29	**5.00**	**0.00**	2.107	2.389	4.771	5.000	0.001	0.468	0.965	1.471

T11(6-9)	**1.10**	**0.9**	1.100	1.097	0.933	1.100	0.901	0.966	0.996	0.965
T12(6-10)	**1.10**	**0.9**	0.900	1.067	1.052	1.100	0.998	1.037	1.100	1.100
T15(4-12)	**1.10**	**0.9**	1.100	0.910	1.095	1.100	0.906	0.929	0.932	0.982
T36(28-27)	**1.10**	**0.9**	0.900	0.919	0.932	1.100	0.900	1.027	0.967	1.026
Active Power Loss (MW)			**1.747**	**1.797**	**1.760**	**1.770**	**-**	**-**	**-**	**-**
Voltage Deviation (p.u)			**-**	**-**	**-**	**-**	**0.294**	**0.316**	**0.315**	**0.395**

Table 7. Single objectives simulation results for case-5 and Case-6 (Adapted IEEE 30 bus system).

Control & State variables	**Min**	**Max**	**Case-5**				**Case-6**			
			MFO	**GWO**	**MVO**	**IMO**	**MFO**	**GWO**	**MVO**	**IMO**
PG2(Thermal)	**20**	**80**	20.000	20.000	20.000	61.428	31.831	32.930	30.941	23.852
PG5(Wind)	**0**	**75**	65.299	67.581	64.957	75.000	45.234	44.664	45.326	52.845
PG8(Thermal)	**10**	**35**	35.000	35.000	35.000	35.000	10.000	10.065	10.000	17.025
PG11(Wind)	**0**	**60**	60.000	60.000	60.000	60.000	38.176	37.439	38.826	32.230
PG13(Thermal)	**12**	**40**	25.375	15.714	28.953	33.666	40.000	40.000	40.000	40.000
VG1	**1.10**	**0.95**	0.950	0.950	0.950	1.100	1.100	1.100	1.100	1.100
VG2	**1.10**	**0.95**	1.100	1.100	1.100	1.100	1.090	1.088	0.976	1.100
VG5	**1.10**	**0.95**	1.100	1.100	1.100	1.100	1.071	1.077	1.071	1.100
VG8	**1.10**	**0.95**	1.100	1.100	1.100	1.100	1.096	1.089	1.098	1.100
VG11	**1.10**	**0.95**	1.100	1.100	1.100	1.100	1.100	1.100	1.100	1.100
VG13	**1.10**	**0.95**	1.100	1.100	1.100	1.100	1.100	1.081	1.100	1.100
QC10	**5.00**	**0.00**	0.099	0.696	2.058	5.000	5.000	1.768	4.550	0.370
QC12	**5.00**	**0.00**	4.865	1.898	4.049	5.000	1.383	0.766	0.734	5.000
QC15	**5.00**	**0.00**	3.328	0.202	2.886	5.000	5.000	2.398	3.311	1.073
QC17	**5.00**	**0.00**	5.000	4.443	4.629	5.000	2.759	2.055	0.107	1.808
QC20	**5.00**	**0.00**	5.000	2.067	1.249	5.000	5.000	0.218	4.936	2.355
QC21	**5.00**	**0.00**	5.000	0.327	1.390	5.000	0.000	3.193	2.490	1.914
QC23	**5.00**	**0.00**	5.000	1.717	3.902	5.000	1.566	0.796	2.218	2.808
QC24	**5.00**	**0.00**	5.000	0.356	0.508	5.000	0.000	4.096	3.812	0.983
QC29	**5.00**	**0.00**	0.020	1.005	0.033	3.944	4.942	1.514	0.015	2.826
T11(6-9)	**1.10**	**0.9**	1.100	0.965	1.100	1.100	1.100	0.919	1.082	1.100
T12(6-10)	**1.10**	**0.9**	1.100	1.019	0.900	1.100	1.079	0.953	0.921	1.100
T15(4-12)	**1.10**	**0.9**	0.900	1.031	1.100	1.100	1.097	1.009	1.016	1.100
T36(28-27)	**1.10**	**0.9**	1.100	0.960	0.900	1.100	1.099	0.973	0.936	1.100
L index			**0.134**	**0.134**	**0.134**	**0.134**	**-**	**-**	**-**	**-**
Total Fuel Cost With Carbon Tax ($/hr)			**-**	**-**	**-**	**-**	**697.703**	**697.857**	**698.138**	**705.190**

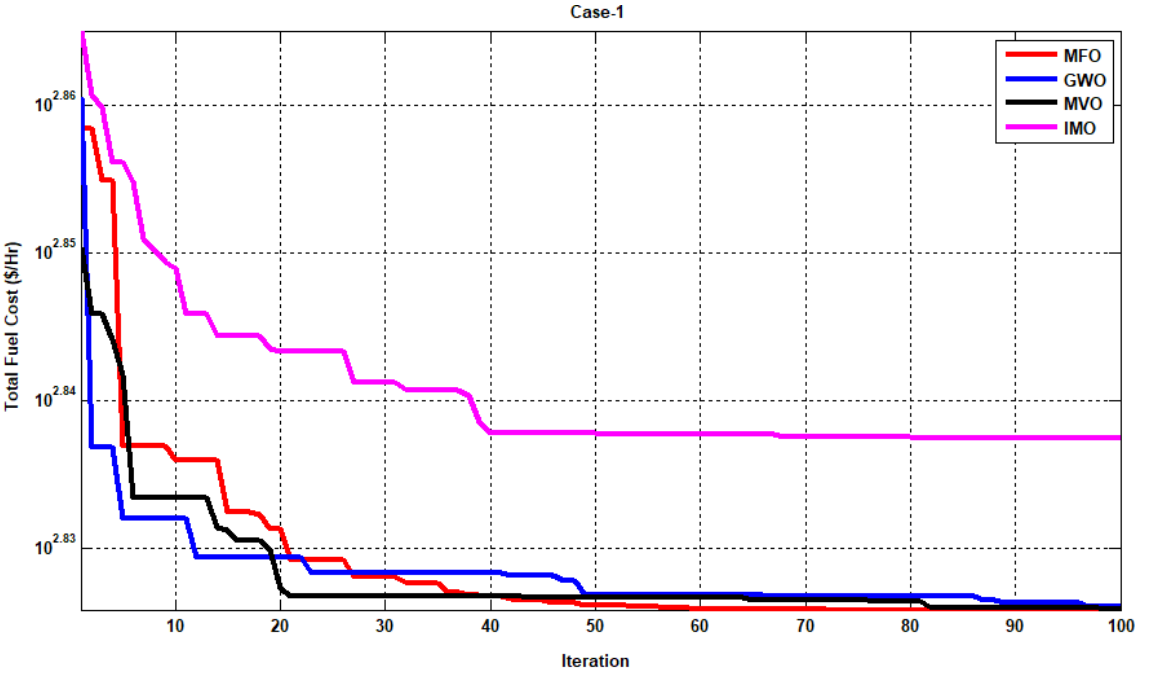

Fig. 7. Convergence characteristics of total fuel cost minimization with two wind power plants.

5.2 Scenario-2 (Multi-objective OPF with wind-thermal power plants)

The multi-objective optimization problems that is two objectives, three objectives and four objectives with case-7 to case-11 are optimized simultaneously with all four algorithms. With fuzzy decision technique, the tradeoff of best compromise solution is illustrated in Fig. 8 to Fig. 10. The results of multi-objective optimal power flow are portrayed in Table 8**.** From the results, it analyzed that the MOMFO approach is one of the techniques for searching the optimal solutions of the multi-objective OPF issue integrating wind-thermal power plants.

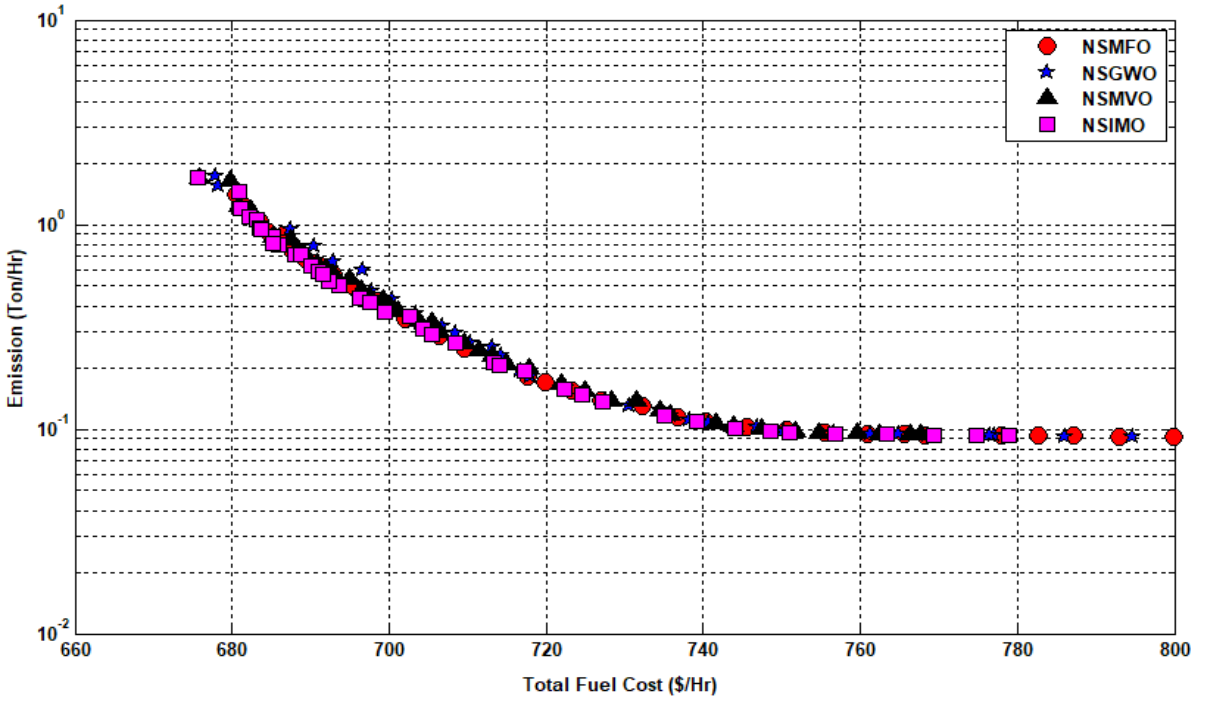

Fig. 8. Pareto front of total fuel cost and emission minimization with thermal-wind power plants.

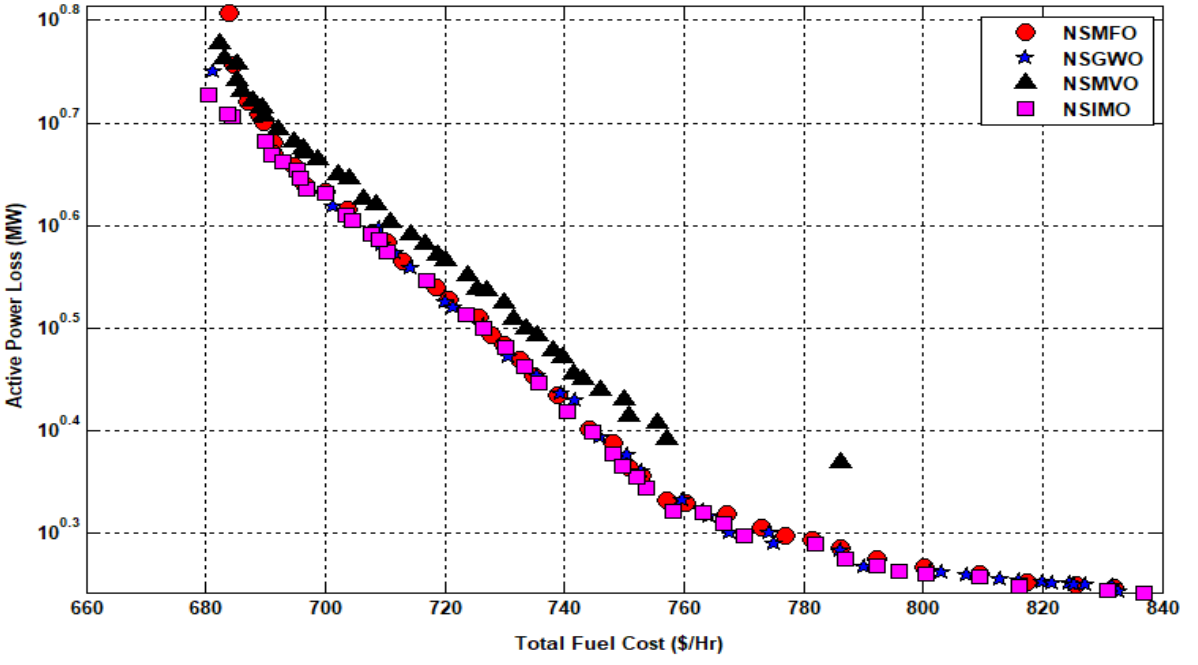

Fig. 9. Pareto front of total fuel cost and active power loss minimization with thermal-wind power plants.

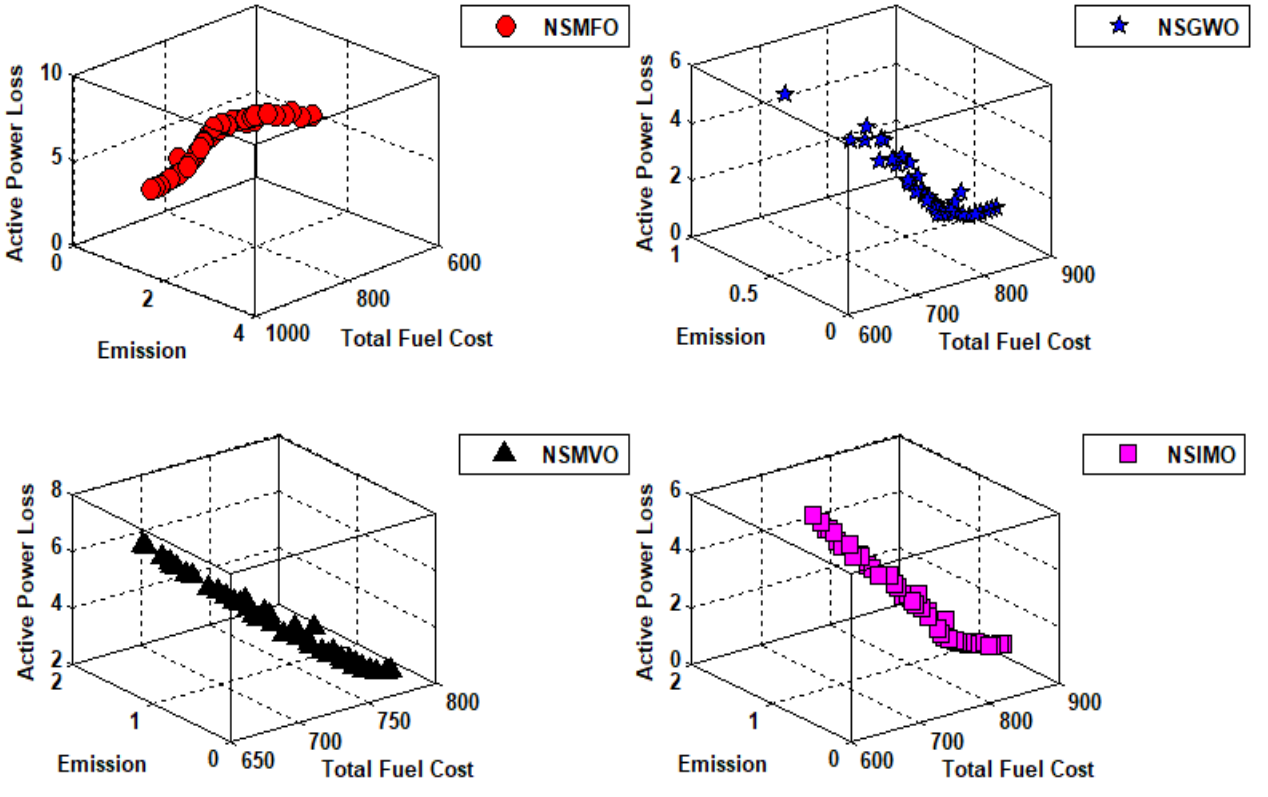

Fig. 10. Pareto front of total fuel cost, Emission and active power loss minimization with wind- thermal power plants.

Table 8. Multi-objectives simulation results obtained for wind-thermal power plants.

Multi-Objectives	MFO	GWO	MVO	IMO
CASE-7				
Total Fuel Cost ($/hr)	**702.026**	**700.309**	**697.637**	**697.652**
Emission (Ton/hr)	**0.344**	**0.431**	**0.443**	**0.414**
CASE-8				
Total Fuel Cost ($/hr)	**727.794**	**726.439**	**720.058**	**733.418**
Active Power Loss (MW)	**3.113**	**3.182**	**3.689**	**2.906**
CASE-9				
Total Fuel Cost ($/hr)	**732.523**	**738.015**	**719.702**	**737.940**
Emission (Ton/hr)	**0.122**	**0.109**	**0.223**	**0.113**
Active Power Loss (MW)	**3.196**	**2.904**	**4.250**	**2.927**
CASE-10				
Total Fuel Cost ($/hr)	**694.780**	**693.595**	**683.557**	**683.974**
Emission (Ton/hr)	**0.585**	**0.523**	**2.044**	**1.150**
Voltage Deviation (p.u)	**0.527**	**0.460**	**0.451**	**0.425**
CASE-11				
Total Fuel Cost ($/hr)	**721.415**	**736.263**	**689.020**	**714.091**
Emission (Ton/hr)	**0.172**	**0.353**	**0.865**	**0.242**
Voltage Deviation (p.u)	**0.690**	**0.521**	**0.707**	**0.528**
Active Power Loss (MW)	**3.768**	**4.958**	**5.606**	**3.955**

6. CONCLUSION

This paper proposes the techno-economic analysis of single and Multi-Objective Optimal Power Flow (MOOPF) issue containing wind-thermal power plants with the moth flame optimizer. The stochastic wind power plants are modelled as Weibull probability density function. The performances are compared with recently available optimization technique. From the obtained result, it is concluded that the suggested MOMFO accomplishes improved quality and additionally feasible solutions for each situation of optimal power flow and has better convergence compare to other algorithms. So finally, it is shown that with a non-dominated sorting method, MOMFO can be proficiently utilized for solving small and large optimal power flow issues by incorporating wind-thermal power plants.

LIST OF NOMENCLATURE

OPF	Optimal Power Flow
TG	Thermal Generator
WG	Wind Generator
ISO	Independent System Operator
PDF	Probability Density Function
BCS	Best Compromise Solution
MOMFO	Multi-Objective Moth Flame Optimization
MOOPF	Multi-Objective Optimal Power Flow
MFO	Moth Flame Optimization
GWO	Grew Wolf Optimization
MVO	Multi Verse Optimization
IMO	Ion Motion Optimization
P_{TGi}	Power output of i^{th} thermal unit.
$P_{ws,j}$	Scheduled power from j^{th} wind power unit
$P_{wav,j}$	Actual available power from j^{th}wind power unit
g_j	Direct cost coefficient for j^{th} wind power unit
$K_{Rw,j}$	Reserve cost coefficient for overestimation of wind power from j^{th}unit
$K_{Pw,j}$	Penalty cost coefficient for underestimation of wind power from j^{th}unit
C_{tax}	Carbon tax in $/Tonne
$f_v(v)$	Probability of wind speed v m/s
p_{wr}	Rated output power of a wind turbine

c,k	Weibull PDF scale and shape parameters respectively
P_{loss}	Real power loss in the grid
VD	Cumulative voltage deviation in a grid

REFERENCES

[1] Carpentier, "**Optimal Power Flows Uses, Methods, and Developments**", *Proceeding. IFAC Conference*, Vol. 18, no.7, pp.11-21, 1985.

[2] K. S. Pandya and S. K. Joshi, "**A Survey of Optimal Power Flow Methods,**" *Journal of Appl. Inf. Technol.*, Vol. 4, No.5, pp. 450–458, 2005.

[3] D. H. Wolpert and W. G. Macready, "**No Free Lunch Theorems for Optimization,**" *IEEE Trans. Evol. Comput.*, Vol. 1, pp. 67–82, 1997.

[4] M. M. A. M. Abido, "**Optimal Power Flow Using Particle Swarm Optimization**," *Journal of Electr. Power Energy Syst.*, Vol. 24, No.7, pp. 563–571, 2002.

[5] M. A. Abido, "**Optimal Power Flow using Tabu Search Algorithm**," *Electr. Power Components Syst.*, Vol. 30, No.5, pp. 469–483, 2002.

[6] G. B. Ghanizadeh, A. J. Mokhtari, G., Abedi, M., Gharehpetian, "**Optimal Power Flow Based on Imperialist Competitive Algorithm,**" *Int. Rev. Electr. Eng.*, Vol.6, pp. 4-12, 2011.

[7] H. R. E. H. Bouchekara, A. E. Chaib, M. A. Abido, and R. A. El-Sehiemy, "**Optimal power flow using an Improved Colliding Bodies Optimization algorithm,**" *Appl. Soft Comput.*, Vol. 42, pp.119–131, 2016.

[8] H. R. E. H. Bouchekara, "**Optimal Power Flow using Black-Hole-Based Optimization Approach,**" Appl. Soft Comput. Vol. 24, pp.879–888, 2014.

[9] Roy Ranjit, Jadhav HT, "**Optimal power flow Solution of Power System Incorporating Stochastic Wind Power using Gbest Guided Artificial Bee Colony Algorithm**." *Int Journal of Electr. Power Energy Syst.*, Vol. 64, pp.562–578, 2015.

[10] Panda Ambarish, Tripathy M. "**Optimal Power Flow Solution of Wind Integrated Power System Using Modified Bacteria Foraging Algorithm.**" Int. *Journal of Electr. Power Energy Syst.*, Vol. 54, pp.306–314, 2014.

[11] Panda Ambarish, Tripathy M. "**Security Constrained Optimal Power Flow Solution of Wind-Thermal Generation System using Modified Bacteria Foraging Algorithm**." *Energy*, Vol. 93, pp.816–827, 2015.

[12] Shi L, Wang C, Yao L, Ni Y, Bazargan M. "**Optimal Power Flow Solution Incorporating Wind Power**." *IEEE Syst. Journal*, Vol. 6, No. 2, pp. 233–241, 2012.

[13] Jabr RA, Pal BC. "**Intermittent Wind Generation in Optimal Power Flow Dispatching**." *IET Gener. Transm. Distrib.*, Vol. 3, No.1, pp. 66–74, 2009.

[14] Mishra, S., Yateendra Mishra, and S. Vignesh. "**Security Constrained Economic Dispatch Considering Wind Energy Conversion Systems.**" *IEEE Power and Energy Society General Meeting*, 2011.

[15] Zhou Wei, Peng Yu, Sun Hui. "**Optimal Wind–Thermal Coordination Dispatch based on Risk Reserve Constraints.**" *Europ.Transact. Elect. Power*, Vol. 21, No. 1, pp.740–756, 2011.

[16] Dubey Hari Mohan, Pandit Manjaree, Panigrahi BK, "**Hybrid Flower Pollination Algorithm with Time-Varying Fuzzy Selection Mechanism for Wind Integrated Multi-Objective Dynamic Economic Dispatch**". *Renewable Energy*, Vol. 83, pp. 188–202, 2015.

[17] Tazvinga Henerica, Zhu Bing, Xia Xiaohua. "**Optimal Power Flow Management for Distributed Energy Resources with Batteries**." *Energy Convers. Manage*, Vol.102, pp. 104–10., 2015.

[18] Kusakana Kanzumba. "**Optimal Scheduling for Distributed Hybrid System with Pumped Hydro Storage.**" *Energy Convers. Manage*. Vol. 111, pp. 253–60, 2016.

[19] P. P. Biswas, P.N.Suganthan, G.A.J.Amartunga, "**Optimal Power Flow Solutions Incorporating Stochastic Wind and Solar**." *Energy conversion and management*, Vol. 148, pp. 1194-1207, 2017.

[20] S.Mirjalili, "**Moth-flame Optimization Algorithm: A Novel Nature-Inspired Heuristic Paradigm,**" *Knowledge-Based Syst*., Vol. 89, pp. 228–249, 2015.

[21] V.Savsani, M.A.Tawhid, "**Non-Dominated Sorting Moth Flame Optimization (NS-*MFO) for multi-objective problems*.**" *Engineering Applications for Artificial Intelligence*, Vol. 63, pp. 20–32, 2017.